Experiment and CFD Analysis of Plain Seal, Labyrinth Seal and Floating Ring Seal on Leakage Performance

Yunseok Ha[1,2], Yeongdo Lee[1,2], Byul An[1,2], and Yongbok Lee[1,2(✉)]

[1] Clean Energy Research Division, Korea Institute of Science and Technology, 5, Hwarangno 14-Gil, Seongbuk-Gu, Seoul 02792, South Korea
lyb@kist.re.kr

[2] Division of Energy and Environment Technology, University of Science and Technology, 217, Gajeong-Ro, Yuseong-Gu, Daejeon 34113, South Korea

Abstract. This paper investigates the leakage characteristic of a non-contact cryogenic seal applied through experiment and CFD analysis. Plain seal (PS), labyrinth seal (LS), and floating ring seal (FRS) were designed for leakage performance test of cryogenic environment. ANSYS Fluent (18.2) was used for creating the flow field of the sealing unit for leakage performance analysis. In order to validate the CFD analysis results, the leakage experimental performance test was also conducted in a cryogenic environment. To create a cryogenic environment, liquid nitrogen (83K) was injected into the test chamber at 0.5 bar, and the test time for each seal was 5,000 s. The results show that among the three types of seals, the FRS had the smallest leakage and the amount of leakage converged quickly. It was confirmed that the largest turbulent kinetic energy was generated when an FRS was used. Also, FRS effectively reduced leakage compared to PS and LS due to the characteristic that clearance changes according to pressure difference. After the leakage performance test, the wear characteristic according to the seal shape was analyzed through surface roughness measurement. In the case of PS, the wear of the surface progressed considerably more than the FRS. Inadequate fluttering adversely affects the wear and leakage performance of the seal. It was found that the wear of PS due to thermal contraction accelerated the friction, and in contrast, the FRS had less friction even with thermal contraction.

Keywords: Cryogenic · Seal · Leakage · CFD · Wear

Nomenclature:

PS	Plain seal
LS	Labyrinth seal
FRS	Floating ring seal
T_{seal}	Seal thickness
H_{seal}	Seal height
T_{LS}	Labyrinth seal thickness
H_{LS}	Labyrinth seal height

T_{FRS} Floating ring seal thickness
F_{total} Total force acting on floating ring seal
F_{top} Top side force acting on floating ring seal
F_{bottom} Bottom side force acting on floating ring seal
A_{top} Top side area of floating ring seal
A_{bottom} Bottom side area of floating ring seal
$\bar{u}, \bar{p}$ Reynolds-averaged flow velocity and pressure
ρ Fluid density
η Dynamic viscosity
$\overline{f_D}$ Additional body forces
τ^{RS} Reynolds stresses

1 Introduction

In turbomachinery applied to cryogenic environments, the sealing unit is a crucial part that directly affects the stability and operating efficiency of the system. Unlike room temperature, the cryogenic sealing unit has many factors to consider. The material of the cryogenic seal is non-isotropic, brittleness, thermal contraction, thermal conductivity, etc., to prevent damage caused by the low-temperature effect. Materials should be selected by considering many factors [1]. In addition, a rapid temperature change in the cryogenic fluid can cause a phase change in the working fluid, which can change the leakage and dynamic characteristics of the seal [2]. In this way, various studies have been conducted to understand the flow characteristics of the working fluid inside the seal in a cryogenic environment, such as the cavitation phenomenon due to the two-phase occurrence according to the seal type as well as the damage due to the thermal contraction of the cryogenic seal.

Ma, Y., et al. [3] presented a CFD model that comprehensively considered heat transfer, cavitation, and evaporation to identify the accurate flow characteristics of the cryogenic fluid and applied it to a two-stage mechanical sealing unit. Through this, it was possible to accurately predict the trend of turbulent flow and phase change occurring in the seal cavity, and it was found that the performance of the impeller had a direct effect depending on the seal's performance. Han, L., et al. [4, 5] analyzed the cavitation phenomenon occurring in the flow inside the labyrinth seal (LS) cavity through the pressure model of the liquid-phase flow. A plain seal (PS) in shape to a plain journal bearing is a mechanism that simply generates flow turbulence and reduces leakage, whereas the LS can effectively reduce leakage by confining the working fluid in the cavity and increasing the turbulence effect. However, since the LS has the possibility of causing dynamic instability of the turbomachinery, a dynamic characteristic analysis must be accompanied. It was confirmed that the cavitation phenomenon occurring in the cryogenic environment greatly affected the LS leakage flow and the geometry parameters such as tooth length and height of the LS. Anbarsooz, M., et al. [6] and Bae, J.-H., et al. [7] conducted a CFD analysis on the floating ring seal (FRS), which can reduce the leakage of working fluid by actively finding the optimal eccentric position according to the rotor position. In the clearance between the FRS and the rotor surface, the same hydrodynamic force as in the fluid film bearing is generated in the radial direction, so

the FRS moves toward the center of the rotor, and the FRS moves until the frictional force of the support ring surface and the hydrodynamic force are balanced. It is fixed in that position and acts like a PS with an arbitrary eccentricity. Huo, C., et al. [8] and Jin, Z., et al. [9] analyzed the dynamic characteristics of the LS and damper seal, which change according to the operating condition, as well as the leakage flow rate of the cryogenic working fluid, using the rotor whirling model of CFD. In the case of the LS, the effective damping ratio of the seal changes greatly depending on the number of teeth, which affects the system's ability, resulting from the change in the swirl ratio of the downstream.

However, lack of experimental results of the sealing unit in the cryogenic environment for validating the analysis model because it is challenging to construct experimental apparatus for testing the sealing unit in a cryogenic environment. Needs of research validating analysis model using experimental results under various operating conditions. Therefore, this paper performed the seal leakage performance test in a liquid nitrogen environment by changing the existing cryogenic ball bearing test apparatus [10] to validate the seal experiment data and CFD model. The cryogenic seal unit consists of three seals: PS, LS, and FRS, and conducts CFD analysis and leakage experiments. After the experiment, surface roughness measurement was conducted to determine the wear according to the shape of the seal.

2   CFD Modeling of Sealing Unity in Cryogenic Environment

2.1   Descriptions of Test Apparatus and Seal Geometry

The test apparatus for the cryogenic seal leakage performance test is shown in Fig. 1. Liquid nitrogen in the chamber leaks between the test bearing part and the lubrication system and a stepped labyrinth seal was applied to reduce leakage in this part. According to the seal shape suggested above, the leakage performance test was conducted using the first cavity part. In order to confirm the leakage flow reduction effect according to the seal shape, a downstream hole was made to measure the temperature and pressure, and the temperature of the supporter bearing of the chamber lubrication part was measured. If the leakage reduction effect of the seal is not achieved, a large amount of liquid nitrogen flows into the lubrication system and the supporter bearing temperature (SBT) bearing drops, so the SBT was also used as data to check the seal performance. The seals used in the cryogenic leakage experiment were designed PS, LS, and FRS, as shown in Fig. 2. In the case of FRS, cryogenic seals were designed by dividing the thickness into two cases (1.5T, 2.0T) because, as shown in (1), the total force acting on the FRS depends on the area.

$$F_{total} = F_{top} - F_{bottom} = P_{mixed} \times A_{top} - P_{up} \times A_{bottom} \tag{1}$$

The geometry information on the three types of non-contact seals is depicted in Table 1.
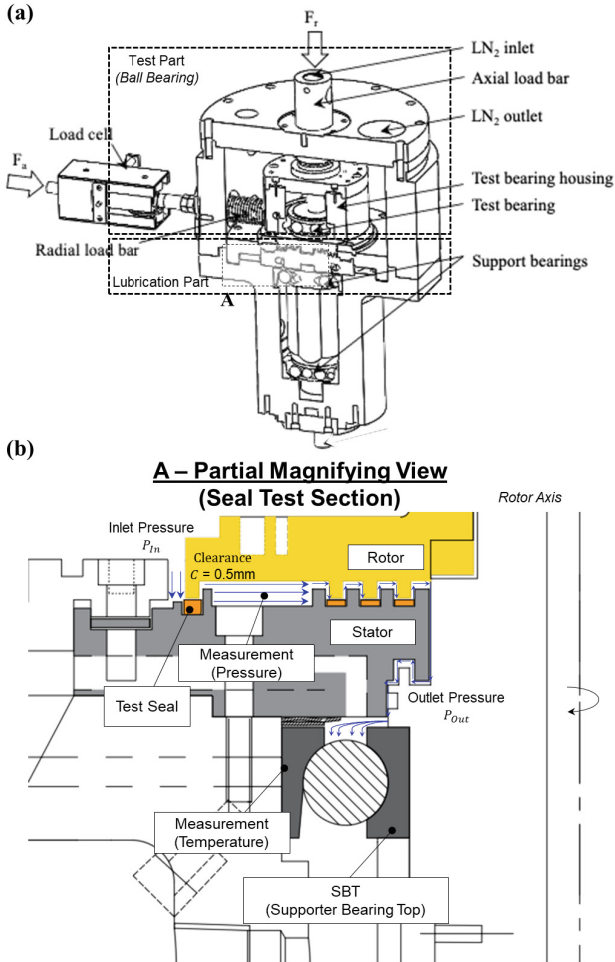
(a)

(b)

Fig. 1. Schematic description of cryogenic performance test apparatus and seal: (a) cryogenic test rig (b) partial magnifying view [10].

2.2   CFD Results of Sealing Unit in the Cryogenic Environment

2D CFD analysis was performed using commercial software ANSYS Fluent (18.2) to analyze the flow characteristics of cryogenic sealing unit leakage. Figure 3 is the mesh for three cases configured using ANSYS meshing. The mesh was constructed to apply the wall function so that the y + value was 30–300 [11]. The mesh was formed using the multi-zone Quad/Tri method, and the mesh was more densely constructed between the seal and the rotor to represent the viscous flow properties better. The Fluent turbulence model determination method is expressed as Eqs. (2), (3) based on the Reynolds Averaged Navier-Stokes (RANS) equation [11].

$$\nabla \cdot \overline{u} = 0 \tag{2}$$

Table 1. Information on design parameters of cryogenic test sealing unit

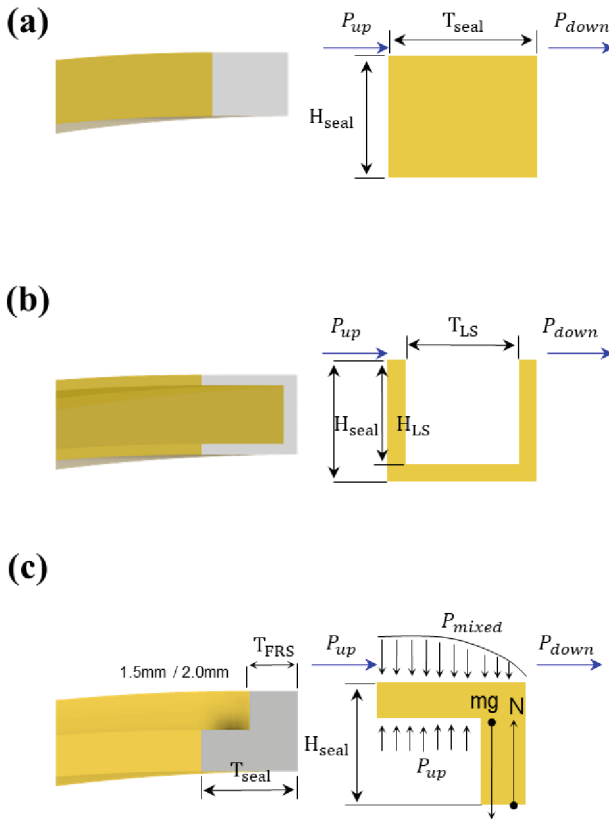| Parameter	Value
Seal Thickness T_{seal},	4 mm
Seal Height, H_{seal}	3.5 mm
LS Thickness, T_{LS}	3 mm
LS Height, H_{LS}	3 mm
FRS Thickness, T_{FRS}	1.5 mm, 2 mm
Material	Copper

Fig. 2. Modeling of cryogenic seal for leakage performance test: (a) PS (b) LS (c) FRS.

$$\frac{\partial \overline{u}}{\partial t} + \rho(\overline{u} \cdot \nabla)\overline{u} = -\nabla \overline{p} + \eta \cdot \overline{u} - \nabla \cdot \tau^{RS} + \overline{f}_D \qquad (3)$$

This paper utilized the standard k-ε model as the turbulence model, and the pressure-based solver and ideal gas equation were applied. Liquid nitrogen from the Fluent
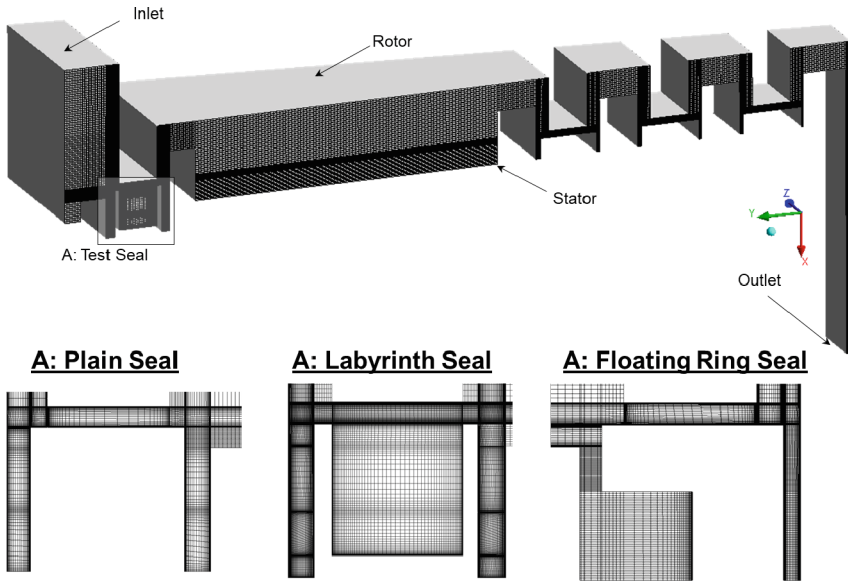
Fig. 3. Mesh generation of cryogenic seal for CFD analysis.

Table 2. Mesh and boundary conditions of CFD model

Mesh Information	Value
Method of meh generation	Multi zone Quad / Tri
Geometry of element	Hexahedral
Boundary conditions	Value
Solver type	Pressure-based / Axisymmetric Swirl
Working fluid	Liquid nitrogen
Inlet pressure	0.5bar
Inlet temperature	83K
Outlet pressure	0.1bar
Rotating speed	3,600rpm

database was used as the working fluid, and the effect of the rotational speed of the rotor was also considered by applying an axisymmetric swirl. A total energy heat transfer model and adiabatic no slip walls were set, and the analysis convergence was determined when the residual terms of k and e and the velocity in the x, and y direction were less than 10^{-5} the detailed mesh boundary conditions listed in Table 2.

Figure 4 shows the cryogenic seal pressure contour and streamline together. It is noteworthy that Fig. 4(c), (d), the flow field of the down streamline in the cavity is greatly affected by the FRS thickness change. The turbulence kinetic energy contour
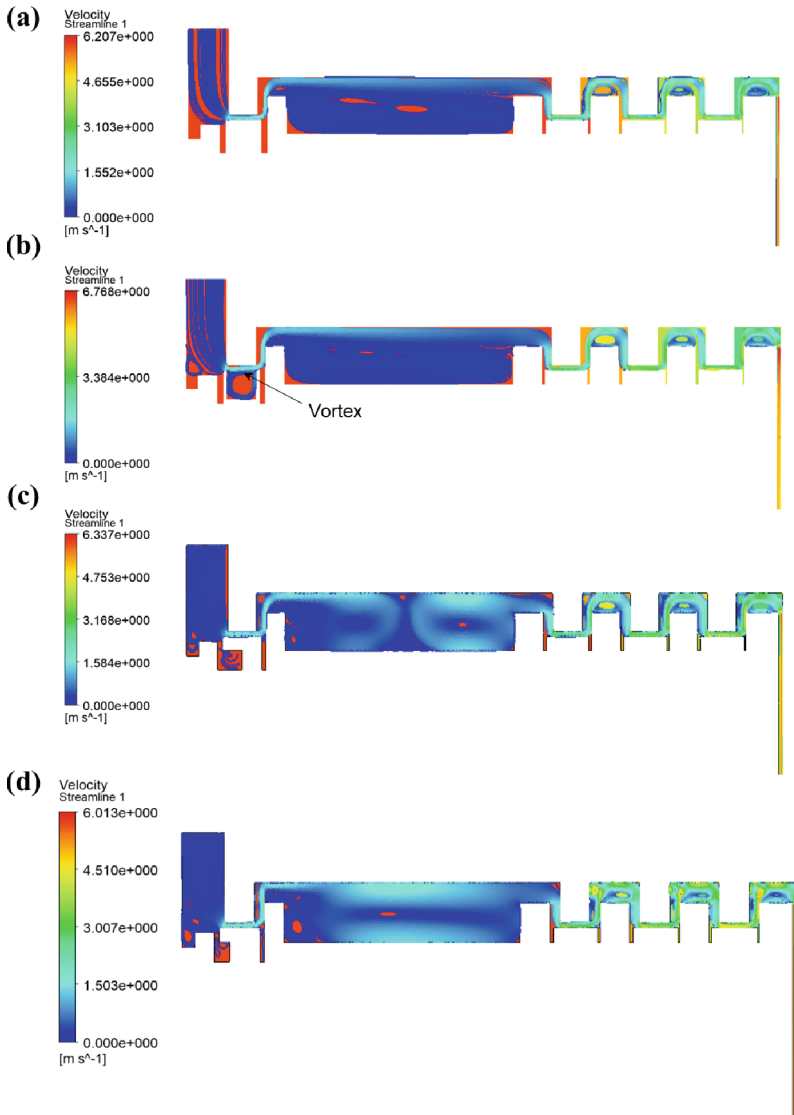
(a)

(b)

Vortex

(c)

(d)

Fig. 4. Graphic contours of pressure and streamline according to cryogenic seal type: (a) PS (b) LS (c) FRS(1.5T) (d) FRS(2T).

is shown in Fig. 5 to confirm the effect of flow change. As seen in Fig. 5, when LS is applied, it can be confirmed that the turbulence kinetic energy is the smallest in the downstream cavity.

On the other hand, in the case of FRS (1.5T), the most considerable amount of downstream kinetic energy occurred, which means that the amount of leakage can be reduced by increasing the flow resistance due to energy dissipation [12]. The data summarizing
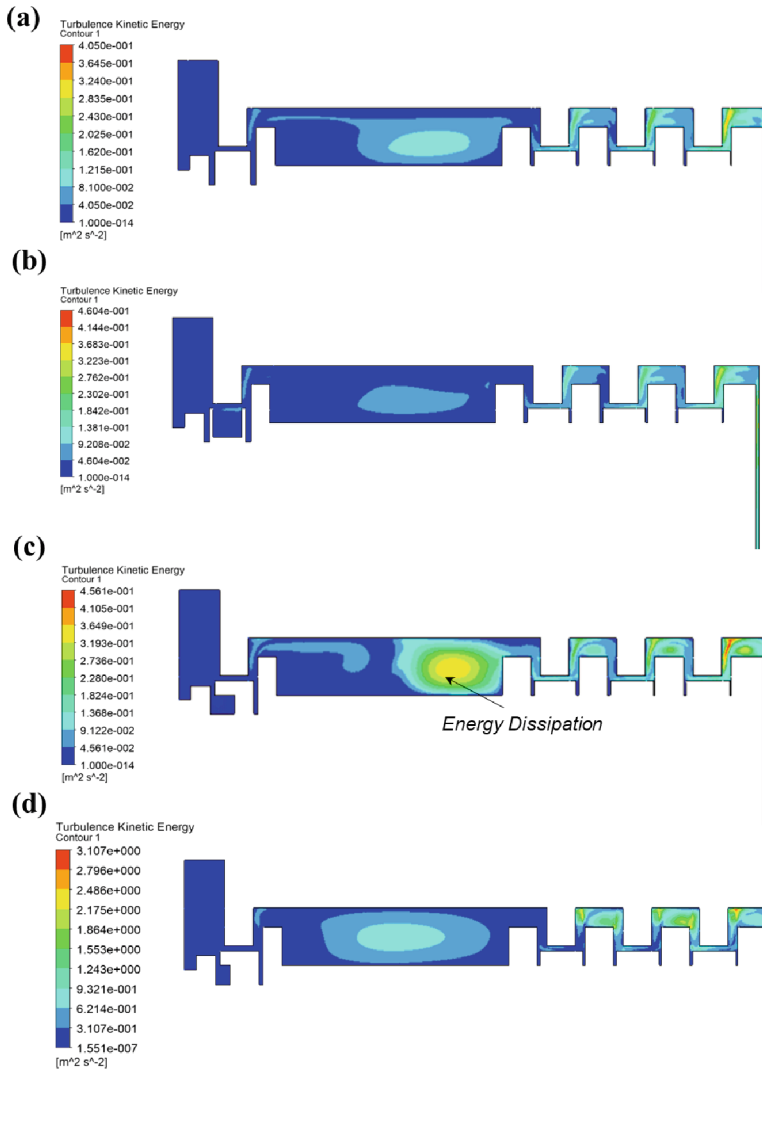
Fig. 5. Graphic contours of turbulence kinetic energy according to cryogenic seal type: (a) PS (b) LS (c) FRS(1.5T) (d) FRS(2T).

the outlet flow rate is listed in Table 3, and as expected in Fig. 5, the FRS (1.5T) case has the lowest outlet flow rate.

Table 3. CFD analysis results of leakage flow rate for sealing unit

Seal Type	Leakage Flow Rate
PS	0.012 kg/s
LS	0.015 kg/s
FRS(1.5T)	0.010 kg/s
FRS(2.0T)	0.011 kg/s

3 Experimental System for Leakage Performance and Roughness Measurement

3.1 Description of Experiment Leakage Performance Test for Sealing Unit

Figure 6 shows a piping and instrumentation diagram capable of conducting a seal leakage performance test in a cryogenic environment. The pressure of liquid nitrogen flowing into the chamber from the liquid nitrogen tank is controlled by a manual valve. To confirm that the liquid nitrogen flowing through the chamber inlet flows at constant pressure and temperature, a liquid nitrogen flow meter, pressure gauge, and thermometer are installed on the inlet pipeline, and an outlet pipeline that can discharge liquid nitrogen inside the chamber due to vaporization is installed. Figure 7 depicts a photograph of a test apparatus for the seal leakage performance test in a cryogenic environment.
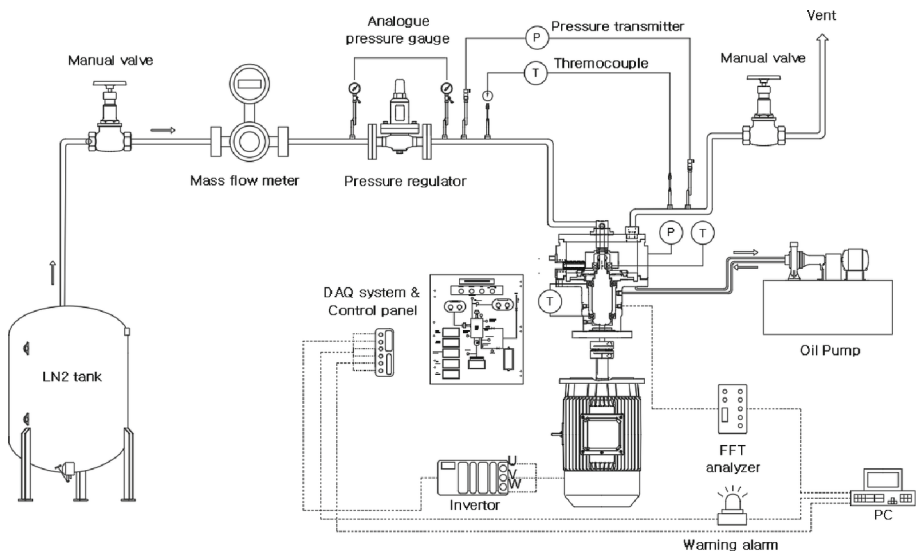

Fig. 6. Piping and instrumentation diagram of the cryogenic facility for the seal on leakage performance [13].
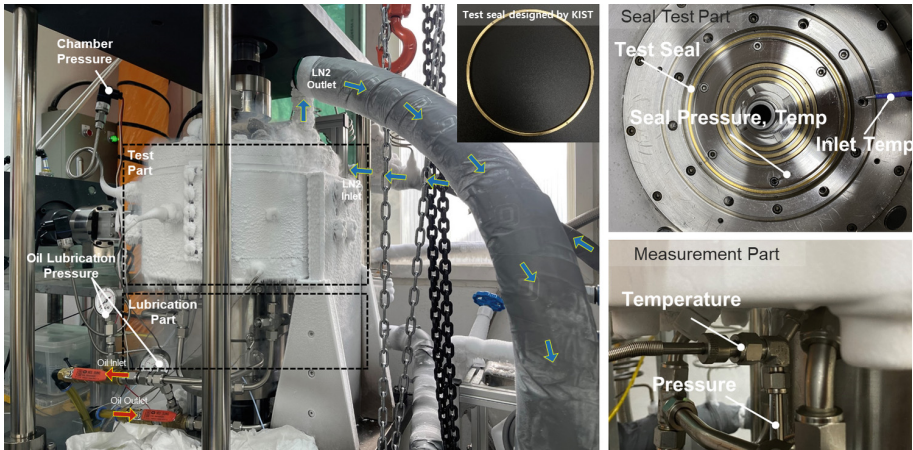
Fig. 7. Photograph of experimental test apparatus for leakage performance test of cryogenic seal type.

Table 4. Cryogenic experimental operating conditions

Parameter	Value
Inlet Pressure	0.5bar
Rotating Speed	3,600rpm
Test Time	5,000s

A hole was made in the seal test part to measure the temperature and pressure according to the seal type. As described above, the SBT of the lubrication system was measured in real-time. As explained in Sect. 2.1, the SBT was used as a criterion of the leakage reduction effect according to the seal shape. This is because the SBT may vary depending on the performance of the test seal. After all, the leak of the seal inserted into the first cavity of the test apparatus is connected to the passage leading to the supporter bearing.

The experiment was conducted after filling the test chamber to a certain level by adjusting the valve so that a constant pressure and flow rate of liquid nitrogen flowed from the LN2 tank. The measurement time was 5,000 s according to the seal type, and the measured data was collected through NI (National Instrumental) DAQ (Data Acquisition) device. The measured data was monitored in real-time through the Labview monitoring program, and the experimental conditions were summarized in Table 4.

3.2 Experimental Results of Leakage Performance Test

Figure 8 shows the temperature measured at the outlet hole according to the seal type. It can be seen that all four cases converge to a specific temperature after 4,000 s.
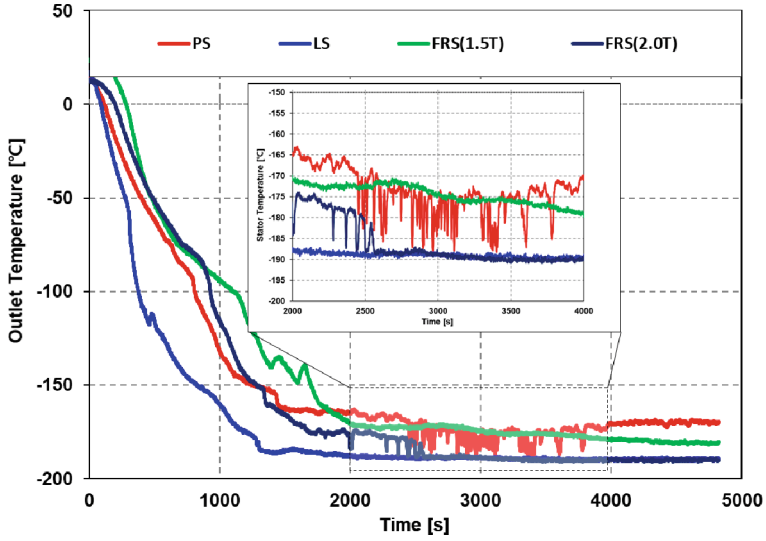
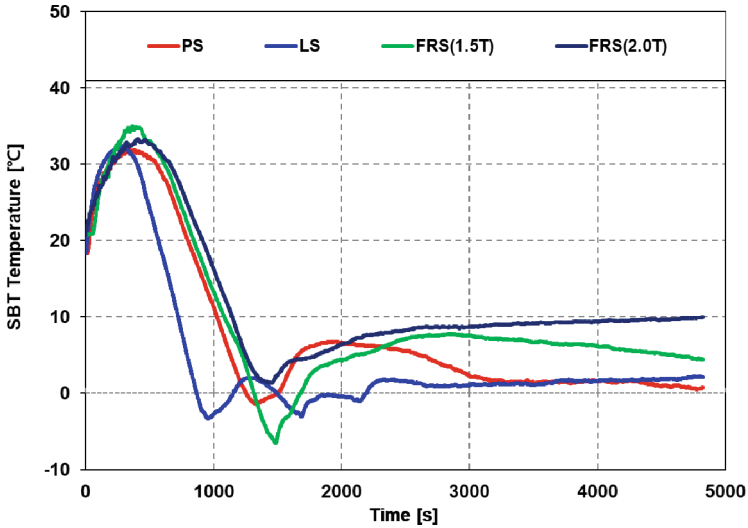**Fig. 8.** Leakage experimental results of outlet temperature depending on seal type.

Fig. 9. Leakage experimental result of SBT depending on seal type.

Among them, in PS, it was confirmed that the temperature fluctuated after the test time was 2,000 s. It is thought that the fluctuation of the temperature was caused by the friction between the rotor and the seal due to the thermal contraction of the seal, and the SBT was checked. Figure 9 is a graph of the SBT data of four cases, and it can be seen that the slope of the SBT changes significantly after 2,000 s, just like the outlet temperature change. In the case of PS, the SBT dropped significantly, while in the case of

FRS (2T), there was a temperature fluctuation in the outlet hole, but the SBT increased. In the case of PS and LS, the temperature convergence tendency is different, but it can be seen that the SBT converges similarly at about 2C˚. Through the SBT experimental data, it can be seen that the FRS effectively reduced the leakage compared to PS and LS, and in the case of FRS, there was a difference from the CFD analysis result. As a result of CFD analysis, there was no significant difference in leakage flow rate, but FRS 2.0T converged to 10C˚ and FRS 1.5T converged to 4 C˚. It is thought that FRS 2.0T effectively reduced leakage compared to 1.5T because the clearance is changed by pressure balance depending on the thickness of FRS. The clearance was fixed and analyzed in the CFD analysis, so it is different from the experimental results.

3.3   Roughness Measurement of Seal Surface for Investigating Wear

Roughness measurement was conducted to check seal surface wear due to friction generated during the leakage performance test. Figure 10 describes the measurement equipment used Taylor HOBSON I60 and the test seal.
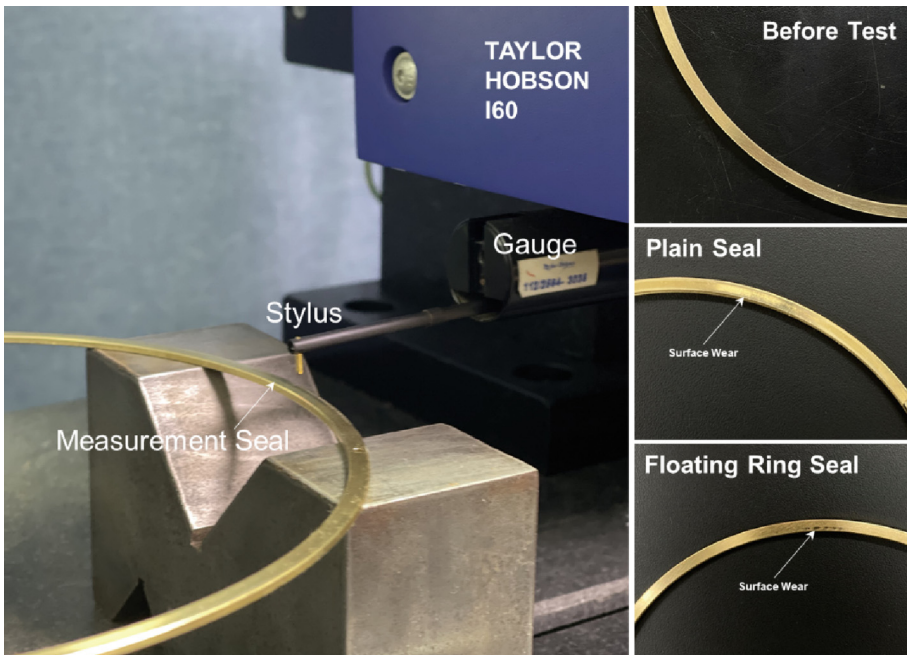

Fig. 10.   Description of a roughness measurement device for investigating seal surface wear.

In the case of LS, the teeth are so thin that it is impossible to measure with current equipment, so the seal surface before the leakage performance test and the surface of PS and FRS after the test were measured, and the details are summarized in Table 5 of the measurement conditions.

Table 5. Specification of measurement device and method

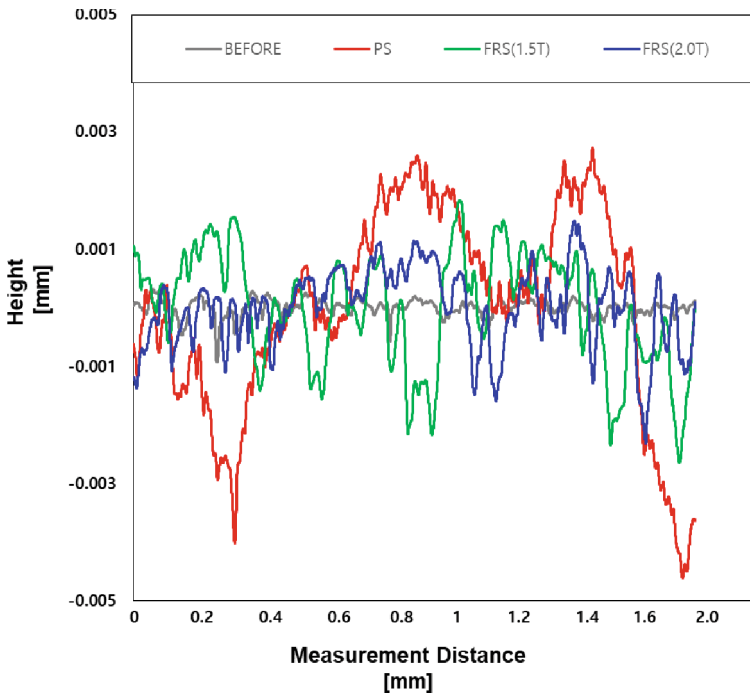| Specification of measurement device	Value
Vertical range	1mm
Resolution	16nm
Horizontal traverse	200mm
Straightness error	0.5um
Data spacing	0.125um
Measurement method	Value
Measurement range	2mm
Data interval	1.25um

Fig. 11. Results of surface roughness according to seal type.

Figure 11 is the roughness measurement result, and it can be confirmed that the roughness Ra of PS was measured larger than FRS. The Ra value of PS was measured to be about 70% larger than that of FRS and the detailed information listed in Table 6. As shown in Fig. 8, the fluctuation of outlet temperature during the measurement period is thought to have caused continuous friction on the seal surface. In the case of plain seal, clearance change between the rotor and seal due to thermal contraction may occur, and

wear may progress. In the case of FRS, even if thermal contraction occurs, clearance is changed due to pressure balance, so it can be seen that less friction of roughness has occurred.

Table 6. Results of roughness measurement for sealing unit

Parameter	Ra Value
Before experiment	0.1063um
PS	1.3558um
FRS(1.5T)	0.7994um
FRS(2.0T)	0.5297um

4   Conclusion

In this study, CFD analysis and experiments were conducted to understand the leakage characteristics of the sealing unit in a cryogenic environment. For the sealing unit, PS, LS, and FRS, 3 types of seals were used, and FRS changed the thickness, so a total of 4 types of sealing units were used. As a result of CFD analysis, it was confirmed that FRS reduced the amount of leakage by effectively generating turbulent kinetic energy in the cavity space compared to PS and LS. In the experiment, the leakage reduction effect of the seal was used as a standard by using the SBT data of the lubrication system. As a result of the experiment, as in the CFD analysis, the SBT was measured to be high in the two cases of FRS, and it was confirmed that the SBT of FRS (2.0T) effectively reduced leakage compared to FRS (1.5T). To confirm the outlet temperature fluctuation, the sealing unit roughness was measured after the experiment, and it was confirmed that PS had greater wear than FRS. This is thought to be wear caused by thermal contraction due to low temperature changing the clearance of the seal, and it was confirmed that the characteristics of FRS can reduce the wear caused by thermal contraction. In future studies, we plan to analyze the flow characteristics generated in the cryogenic environment by conducting an analysis that considers the clearance change of FRS, which needs to be reflected in this study.

Appendix. Sensor Uncertainty

In order to confirm the reliability of the results of this cryogenic leakage experiment, an uncertainty analysis of the sensor was performed. For the uncertainty of the sensor, the same sensor used in the experiment of Choe, B., et al. [14] was used, and Eq. (4)

represents the uncertainty of the entire measurement system.

$$U = \{\left(\frac{\partial A}{\partial x_1}u_1\right)^2 + \left(\frac{\partial A}{\partial x_1}u_2\right)^2 + \cdots + \left(\frac{\partial A}{\partial x_1}u_n\right)^2\}^{\frac{1}{2}} \tag{4}$$

where U is the uncertainty of the entire system $A = (x_1; x_2; \cdots; x_n)$ and $u_1; u_2; \cdots; u_n$ were uncertainty of each sensor. The uncertainty of cryogenic leakage experiment is 1.14% and is the result obtained by using Eq. (4) (pressure sensor: $\pm$ 0.15%, thermocouple sensor: $\pm$ 1.50%, flow meter: $\pm$ 0.05%).

References

1. Jia, L.X.: Experimental and theoretical studies of cryogenic sealing. Florida Atlantic University (1996)
2. San Andres, L., Yang, Z., Childs, D.W.: Thermal effects in cryogenic liquid annular seals—Part II: Numerical solution and results (1993)
3. Ma, Y., et al.: Numerical investigation on sealing behaviors of an extremely high-speed two-stage impellers structure in cryogenic rockets. Asia-Pac. J. Chem. Eng. **13**(5), e2229 (2018)
4. Han, L., et al.: Theoretical modeling for leakage characteristics of two-phase flow in the cryogenic labyrinth seal. Int. J. Heat Mass Transf. **159**, 120151 (2020)
5. Han, L., et al.: Theoretical leakage equations towards liquid-phase flow in the straight-through labyrinth seal. Journal of Tribology **144**(3) (2022)
6. Anbarsooz, M., et al.: Effects of the ring clearance on the aerodynamic performance of a CO2 centrifugal compressors annular seal: A numerical study. Tribol. Int. **170**, 107501 (2022)
7. Bae, J.-H., et al.: Numerical and experimental study of nose for LOx floating ring seal in turbopump. Aerospace **9**(11), 667 (2022)
8. Huo, C., et al.: Influence of tooth geometrical shape on the leakage and rotordynamic characteristics of labyrinth seals in a cryogenic liquid turbine expander. Int. J. Refrig **145**, 105–117 (2023)
9. Jin, Z., et al.: A comparison of static and rotordynamic characteristics for three types of impeller front seals in a liquid oxygen turbopump. J. Eng. Gas Turbines Power **145**(3), 031025 (2023)
10. Lee, Y.B., Choe, B.S., Lee, J.K., Ryu, S.J., Lee, B.K.: Bearing Test Apparatus for Testing Durability of Bearing. U.S. Patent No. 9714883 (2016)
11. Manual, U.: ANSYS FLUENT 12.0. Theory Guide (2009)
12. Greifzu, F., et al.: Assessment of particle-tracking models for dispersed particle-laden flows implemented in OpenFOAM and ANSYS FLUENT. Engineering Applications of Computational Fluid Mechanics **10**(1), 30–43 (2016)
13. Kwak, W.I.: Failure criteria and life model to verify the reliability of cryogenic rolling bearing. University of Science and Technology (2023)
14. Choe, B., et al.: Experimental study on dynamic behavior of ball bearing cage in cryogenic environments, Part I: Effects of cage guidance and pocket clearances. Mech. Syst. Signal Process. **115**, 545–569 (2019)